RESEARCH ARTICLE





Numerical modeling of groundwater-driven stream network evolution in low-relief post-glacial landscapes

Cecilia Cullen 💿 | Alison M. Anders 💿 | Jingtao Lai 💿 | Jennifer L. Druhan 💿

Department of Geology, University of Illinois, Urbana, Illinois, USA

Correspondence

Cecilia Cullen, Illinois State Water Survey, 2204 Griffith Dr., MC-674, Champaign, IL 61820-7463, USA. Email: ccullen3@illinois.edu

Present address

Cecilia Cullen, Illinois State Water Survey, Champaign, Illinois, USA

Jingtao Lai, GFZ German Research Centre for Geosciences, Potsdam, Germany

Funding information

National Science Foundation, Grant/Award Numbers: NSF EAR 13-31906 Critical Zone Observatory for Int, NSF EAR 16-56935 Collaborative Research, Drainage

Abstract

In the low-relief post-glacial landscapes of the Central Lowlands of the United States, fluvial networks formed and expanded following deglaciation despite the low slopes and large fraction of the land surface occupied by closed depressions. Low relief topography allows for subtle surface water divides and increases the likelihood that groundwater divides do not coincide with surface water divides. We investigate how groundwater transfer across subtle surface water divides facilitates channel network expansion using a numerical model built on the Landlab platform. Our model simulates surface and subsurface water routing and fluvial erosion. We consider two end-member scenarios for surface water routing, one in which surface water in closed depressions is forced to connect to basin outlets (routing) and one in which surface water in closed depressions is lost to evapotranspiration (no routing). Groundwater is modeled as fully saturated flow within a confined aquifer. Groundwater emerges as surface water where the landscape has eroded to a specified depth. We held the total water flux constant and varied the fraction of water introduced as groundwater versus precipitation. Channel growth is significantly faster in routing cases than no-routing cases given identical groundwater fractions. In both routing and no-routing cases, channel expansion is fastest when $\sim\!30\%$ of the total water enters the system as groundwater. Groundwater contributions also produce distinctive morphology including steepened channel profiles below groundwater seeps. Groundwater head gradients evolve with topography and groundwater-fed channels can grow more quickly than channels with larger surface water catchments. We conclude that rates of channel network growth in low-relief post-glacial areas are sensitive to groundwater contributions. More broadly, our findings suggest that landscape evolution models may benefit from more detailed representation of hydrologic processes.

KEYWORDS

fluvial networks, groundwater, Landlab, landscape evolution, post-glacial

1 | INTRODUCTION

River channels initiate and expand in unchannelized areas across a range of landscapes including marine terraces (Anderson et al., 1999), lava flows (Simon, 1999), and areas blanketed by glacial sediment (Pillans, 1985; Ruhe, 1952). In low relief areas with many closed depressions, such as the formerly glaciated Central Lowlands physiographic province of North America (Fenneman & Johnson, 1946), the processes by which channel networks grow are enigmatic. Theoretical

models of stream erosion are driven by slope and discharge (e.g., Whipple & Tucker, 1999), with discharge often approximated as a simple function of drainage area (e.g., Lague, 2013). Observations of the location of channel heads in mature mountainous landscapes suggest a trade-off between slope and discharge as a criterion for channelization (Montgomery & Dietrich, 1995). Therefore, in areas of low slope, greater discharge is expected to be required to drive channel incision than in areas with significant slopes. The post-glacial land-scapes of the Central Lowlands were characterized by low slopes and

contained many closed depressions, which created many small and disconnected surface water catchments, limiting the surface-water derived discharge of incipient channels. The limited slopes and surface water drainage areas make it difficult to explain how channel networks could have expanded in this region.

Nevertheless, the spatial variability in drainage density across the Central Lowlands indicates that channel networks have expanded following deglaciation. Drainage density in areas most recently glaciated 10,000-25,000 years ago is variable, but generally lower than in areas glaciated only during earlier glaciations (Miller et al., 2009; Ruhe, 1952). Lai and Anders (2018) presented numerical models of channel network expansion in an idealized landscape mimicking the post-glacial Central Lowlands. Their model focused on the expansion of channels into a low-relief upland with closed depressions. Channel network expansion was forced by the presence of an incised valley created by glacial meltwater and imposed along one boundary of the domain. Lai and Anders (2018) compared and contrasted models with two different surface water routing scenarios; one which forced all water to be routed out of closed depressions to reach the edge of the domain (routing), and another which allowed surface water introduced to closed depressions and their catchments to be lost to evapotranspiration (no-routing). They found significant differences in the rates and morphologies of channel networks formed in these two scenarios. Channel network evolution was much more rapid in the routing scenario. Channel networks formed in the routing scenario had dendritic planform patterns that were dictated by noise in the initial topography, while channels in the no-routing scenario were straighter, shorter and more closely spaced, having initiated at a preferred spacing along the edge of the incised valley wall. Present topography of the Central Lowlands includes examples of channel networks resembling both scenarios but the overall drainage density of the region is more consistent with the routing scenario being prevalent, leading Lai and Anders (2018) to conclude that the observed channel networks of this region likely required routing of water across the subtle topographic divides.

We build on the work of Lai and Anders (2018) and consider an alternative mechanism for concentrating water to produce discharge sufficient to drive channel incision in a low-relief landscape. Specifically, we consider the potential for groundwater routing across subtle surface water divides to contribute to channel network expansion and assess the impact of such groundwater on rates of channel network growth and morphology. In the most recently glaciated portions of the Central Lowlands, significant fractions of the land surface are observed to be unconnected from large-scale drainage networks. For example, prior to the conversion to intensive agriculture in northern and central Iowa, 44% of the region was occupied by wetlands (Miller et al., 2009), many of which were not connected by surface pathways to externally-draining rivers. Closed depressions were estimated to occupy 40% of the area of the Upper Sangamon River Basin in eastcentral Illinois (Blair et al., 2021), which lies in the heart of the Grand Prairie, an extensive area dominated by wet prairie that was drained and converted to row crop agriculture in the late 19th century (Urban, 2005). Groundwater in low-relief post-glacial areas has been observed to cross subtle topographic divides, for example in the Prairie Potholes of North Dakota (Winter & Rosenberry, 1998), glacial sediments in Wisconsin and Minnesota (Winter et al., 2003), and the sandy glacial lowlands of the Netherlands (De Vries, 1994). Groundwater

springs have been observed to emerge at the interface between unconsolidated sandy glacial sediments and underlying bedrock (Swanson et al., 2009). Additionally, the layered contrasting permeability of glacial sediments (till, glaciolacustrine, glaciofluvial, loess) can favor horizontal groundwater flow paths and groundwater emergence at sedimentological boundaries (Cuthbert, 2006; Smith, 2007). The fact that large fractions of the land surface are disconnected from external drainage networks highlights the potential significance of fluvial discharge originating from groundwater flow across surface water divides. Groundwater redistribution at the regional scale has been recognized as a significant contribution to discharge (Shaller & Fan, 2009) and remains a challenge for modeling hydrology and land-scape evolution.

To numerically model the impact of such groundwater flow on channel network expansion requires a more refined treatment of hydrology than is typical for landscape evolution models, which generally greatly simplify hydrological processes. River discharge is commonly assumed to linearly scale with drainage area (e.g., Anderson, 1994; Beaumont et al., 1992; Tucker & Slingerland, 1994). Moreover, drainage area is frequently calculated using a simple algorithm that forces precipitation falling on every part of the domain to be routed to the edge of the model (O'Callaghan & Mark, 1984). Motivated by observations in low-relief landscapes, we explore the impacts of relaxing these two idealizations (discharge scales with surface drainage area, and, surface water is forced out of closed depressions) in a model integrating the evolution of drainage networks with the underlying groundwater flow field through time.

We explore a relaxation of the simple assumption of a direct scaling of discharge with surface water drainage area. Specifically, we consider a mechanism for decoupling discharge and surface water drainage area via subsurface flow across surface water divides by adding a representation of groundwater flow in a confined shallow aquifer. Groundwater flow is independent of surface topography except where it emerges to become surface water. We specify that this emergence as surface water occurs when and where fluvial erosion has eroded below a specified depth corresponding to the elevation of a confined aquifer. We use our model to assess the morphological signatures of fluvial network evolution driven by the addition of groundwater to surface flow and compare the rates of channel growth as a function of groundwater contribution. A recentlydeveloped Landlab component, Groundwater Dupuit Percolator (Litwin et al., 2020), solves for the water table elevation and groundwater flux to the surface from an unconfined aquifer allowing for investigation of changes in surface and groundwater fluxes and storage during storm events. We are focused on landscape evolution over thousands of years in the specific situation of groundwater transfer across surface water divides. Idealizing this as a confined aquifer allows us to control groundwater input independent of surface topography. Specifically, we envision a source of groundwater from beyond the model domain where infiltration contributes groundwater to a conductive layer at depth. Future work comparing and contrasting groundwater transfer in an unconfined aquifer to our models of a confined aquifer is possible.

In addition to relaxing the association between surface area and river discharge, we explicitly consider surface water transfer through closed depressions. Closed depressions exist in landscapes at a range of spatial scales, commonly occur as artifacts in digital elevation models, and are present in the synthetic initial conditions typical of landscape evolution studies. Many landscape evolution model studies neglect any influence of closed depressions by forcing their integration into externally-draining river networks and counting the drainage area of closed depressions as contributing to the discharge driving fluvial erosion. The occurrence of true closed depressions in low relief landscapes suggests that explicit consideration of the fate of precipitation falling into these features and their catchments is vital to understanding the concentration of discharge and, by association, fluvial incision in these landscapes.

We consider the same two end-member scenarios for surface water routing in the presence of closed depressions used by Lai and Anders (2018): one in which we force connection via surface pathways to externally-draining rivers (routing) and one in which all the precipitation falling on the closed depression and its basin is lost to evapotranspiration (no-routing). In the routing scenarios, we use a lake-filling algorithm implemented by Tucker et al. (2001) which routes water from closed depressions out through the lowest elevation spillway on the basin edge. Two new algorithms, FlowFill (Callaghan & Wickert, 2019) and Fill-Spill-Merge (Barnes et al., 2020), simulate flooding of closed depressions as a function of a specified surface runoff depth and represent an intermediate condition between our scenarios by allowing hydrologic connectivity of a fraction of the closed depressions in a landscape as a function of scale and position. Incorporating one of these algorithms into a model of landscape evolution in the Central Lowlands is a target for future research.

Previous work has examined landscape evolution dominated by groundwater flow in landscapes that experience very little overland flow including sandy post-glacial landscapes in the Netherlands (De Vries, 1976) and a broad, low-relief landscape formed in fluviodeltaic and marine sand in the Florida panhandle (Abrams et al., 2009; Devauchelle et al., 2012; Schumm et al., 1995). Observations indicate that groundwater can mobilize sediment in the subsurface, creating and enlarging pseudo-karst tunnels which may subsequently collapse (Higgins, 1984). This process is referred to as piping or seepage erosion and has been hypothesized to contribute to drainage network expansion in humid regions (Dunne, 1980). Additionally, the emergence of groundwater at the surface can decrease resistance to erosion due to the reduction of granular pressure within the outcropping aquifer (e.g., De Vries, 1976) and the extension of channel heads by undermining of cliff face where groundwater emerges (referred to as sapping) is also observed (e.g., Harrison et al., 2020).

In contrast to these previous efforts, we do not directly represent the processes of seepage erosion or sapping, but instead focus solely on the impact of groundwater as an added contribution to surface water discharge. The increased discharge that results from groundwater emergence as surface water increases the rate of fluvial incision. The only process of erosion we model is that of fluvial incision. We intentionally choose to use this idealized and simple approach because it allows us to focus only on the consequence of additional discharge for driving fluvial incision. This approach offers a novel and important first look at the potential role of groundwater originating from beyond the boundaries of the surface water catchment in driving channel network evolution in low-relief landscapes.

2 | METHODS

We construct a numerical model of the coupled evolution of ground-water head gradients and landscape elevation to document how channel morphology responds to contributions of groundwater and to assess the effect of this groundwater on relative rates of channel head cutting. This model is built using the Landlab software platform (Barnhart et al., 2020; Hobley et al., 2017). Landlab is an open-source, Python-based repository for models of geomorphic phenomena. Users construct landscapes and apply boundary conditions, hydrologic processes, and geologic processes to the domain. These processes are represented and propagated forward in time by modular Landlab components. We use existing Landlab components to set up our model domain and evolve the landscape through time. We build a new component to simulate flow of groundwater and use it to calculate the evolution of the spatial distribution of groundwater hydraulic head in response to changes in the topography through time.

2.1 | Experiment design

We ran our coupled model of fluvial erosion and groundwater head gradients using an initial condition similar to that used by Lai and Anders (2018) (Figure 1). The domain is a 1 km by 1 km square grid with a grid spacing of 10 m. The left edge of the model is fixed at an elevation of 0 m, representing an incised valley, and the remainder of the domain is a 15 m elevation plateau with random noise of up to 1 m, representing the unchannelized upland. The same random noise is applied in all model runs to allow for direct comparison of the growth of specific tributaries under different conditions. We focus on the early evolution of the system before channels extend more than a few hundred meters. Therefore, the figures we show are only of the left half of the domain.

The total water flux into the domain is constant throughout all our simulations at a value of 1e6 m³/yr which is equivalent to a uniform rain rate of 1 m/yr across the entire domain and similar to the modern annual precipitation rates across the Central Lowlands (\sim 500–1250 mm/yr). While holding the total water flux fixed, we vary the fraction of water that enters the domain as groundwater. Groundwater, as described in detail later, enters the right side of the model domain along a fixed flux boundary condition and emerges as surface water where the topography is incised below 10 m elevation.

The remaining fraction of the water is supplied as precipitation distributed uniformly in space and time. In one set of cases (NR: no routing) precipitation falling on closed depressions and their catchments is lost to evapotranspiration and does no work on the landscape. These simulations use the Landlab component Flow-Accumulator with the D8 flow routing algorithm (O'Callaghan & Mark, 1984) to route precipitation falling on each cell to its downstream neighbor via the path of steepest descent. Precipitation falling within the catchment of a closed depression is accumulated at the lowest point in the catchment and not forced to exit the domain. In our second set of cases (R: routing) the precipitation is routed out of closed depressions and forced to exit the domain. In this case the Landlab component DepressionFinderandRouter (Tucker et al., 2001) is used to identify closed depressions and pass their water across surface water divides until it is forced to the edge of the domain.

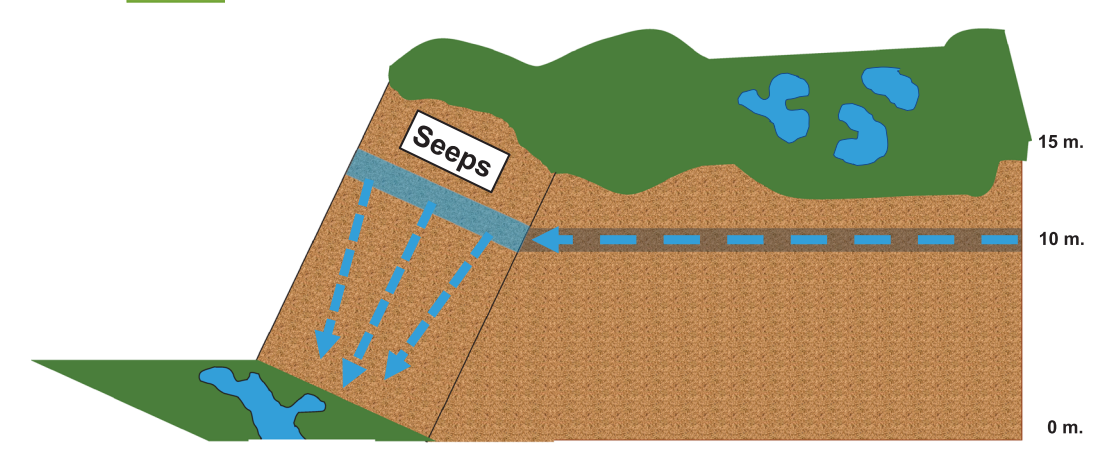


FIGURE 1 A valley is incised to a depth of 15 m below a low-relief upland. Tributaries will evolve to connect the upland to the pre-existing valley. Groundwater moves in a conductive layer (aquifer) from a source outside the domain and beyond the (initial) surface water catchments of the tributaries. A fixed flux of groundwater is fed into the right side of the domain to emerge as surface water where the conductive layer crops out in the landscape at an elevation of 10 m above the valley floor. The entire flux of groundwater is discharged to the first point below 10 m elevation, water is not distributed vertically within the aquifer

TABLE 1 Description of coefficients held constant in the model simulation

Coefficient	Description	Value
K sp	Erosion coefficient from FastscapeEroder component (yr ^{0.5} /m ^{0.5})	0.0001
t	Threshold for erosion in FastscapeEroder, no erosion in the landscape below this value (m/yr)	0.0005
L	Length of each square cell (m)	10
CA	Cross-sectional area of the seep layer (m²)	100
Noise	Random difference, higher and lower, in initial landscape elevation from 15 m at each cell (m)	≥ 1
K gw	Hydraulic conductivity of the seep layer (m/yr)	1,000

Accumulated precipitation is added to emergent groundwater to calculate a surface water discharge at each grid cell. Fluvial erosion is the only process of landscape evolution in our model. The Landlab component FastscapeEroder, based on Braun and Willett (2013) is used to implement fluvial erosion with a timestep of 1000 years Equation 1.

$$E_{\text{Fluvial}} = K_{\text{sp}} \left(R \times A + Q_{\text{gw}} \right)^{0.5} S - t \tag{1}$$

where $K_{\rm sp}$ [L^{-0.5}/T^{0.5}] is a constant, R is the spatially and temporally uniform precipitation rate [L/T], A is contributing drainage area [L²], $Q_{\rm gw}$ is groundwater discharge to the surface [L³/T], S is dimensionless topographic slope and t [L/T] is a threshold below which erosion does not occur. The values of $K_{\rm sp}$ and t are fixed in all experiments (Table 1). We tested the sensitivity of the model to the timestep by comparing one routing and one no-routing case with timesteps of 100 and 10 years to the cases with 1000 years we present here. The modeled landscapes are qualitatively very similar in the number, spacing, length, and profiles of channels for all timesteps. The only observed difference as a function of timestep is the lateral translation of one cell (10 m) of in the location of main channels. We conclude

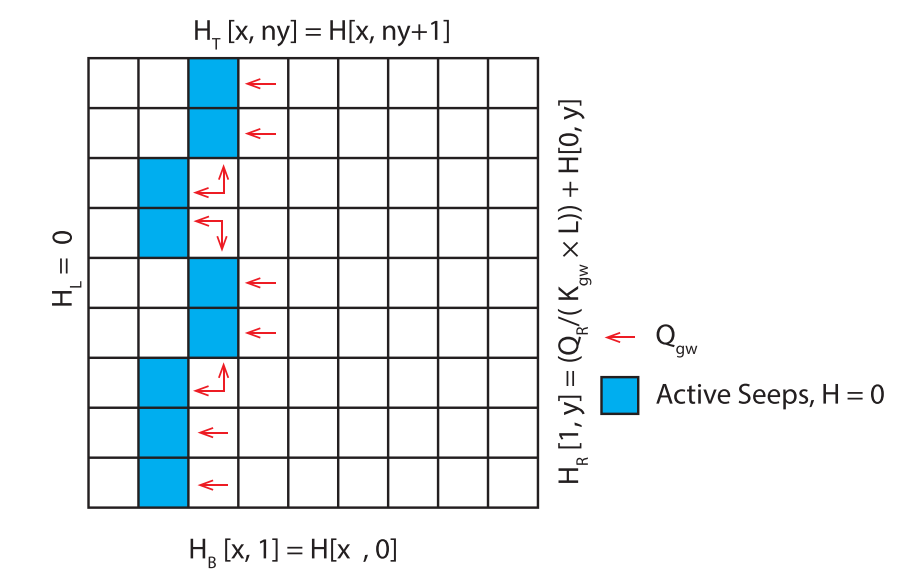
that the more efficient simulations with 1000 year timesteps are sufficient to identify the morphological tendencies of the system.

2.2 | Groundwater model

Our new groundwater component, SeepCharge, simulates the flow and emergence of groundwater and calculates the volumetric groundwater flux (Q_{gw}) that is added to surface water in the fluvial erosion (Equation 1. We begin by envisioning subsurface flow in a confined aguifer driven by a head gradient from a groundwater recharge area outside the domain to an incised trunk valley where the aquifer outcrops (Figure 1). This situation requires a conductive layer in the shallow subsurface with relatively impermeable material below. While this aguifer is assigned an effective thickness and hydraulic conductivity we do not partition the flow within the aquifer to a range of elevations. Instead, the aquifer discharges its entire groundwater flux to surface water at the first cell it encounters which has eroded to below a fixed elevation of 10 m. Where this groundwater emerges, we fix the value of groundwater hydraulic head to 0 m, representing atmospheric pressure. All points in the model domain with elevations below 10 m are assigned hydraulic head values of 0. In our initial condition, a pre-existing truck stream is present along the left edge of the domain, therefore, all groundwater introduced along the right boundary emerges as surface water within the domain throughout the entire simulation. We solve for the steady-state distribution of hydraulic head and the resulting flow field based on a fixed flux of groundwater through the right boundary and no flow boundaries across the top and bottom of the domain assuming fully saturated Darcy flow (Figure 2). This steady-state head field determines how the flux of groundwater entering the right side of the model is distributed among the internal grid cells and along the left boundary where the aquifer outcrops to an incised channel present in the initial condition.

We choose this representation of groundwater flow across surface water divides for its simplicity while acknowledging that in post-glacial landscapes of the Central Lowlands we expect variability in hydrological conductivity, both horizontally and vertically, to be much

FIGURE 2 Schematic of groundwater model with boundary conditions illustrated. The right boundary is a fixed flux of groundwater (Equation 6), the left boundary is a fixed groundwater head of 0 (Equation 3). Top and bottom boundaries are no-flux conditions (Equations 4 and 5). Groundwater emerges as surface water at seep locations illustrated by red arrows. The model domain has more cells than shown in this schematic



more complex. Additionally, we recognize that unsaturated flow in surficial aquifers also introduces groundwater to surface streams in these landscapes. Another complexity is the potential for surface water introduced as precipitation to infiltrate within closed depressions and travel as groundwater to surface streams outside the boundaries of the closed depressions. Surface water–groundwater interaction in the context of the closed depressions of the Central Lowlands is important for understanding the hydrology as well as the nutrient and carbon cycling in these landscapes and is the subject of active model development (e.g., Le et al., 2015., Yan et al., 2019). However, these complications are beyond the scope of this first idealized study of the long-term interactions between channel network evolution and groundwater transit across surface water divides.

We implement this model in Python by discretizing Darcy's Law using a two-dimensional explicit scheme. This scheme calculates the distribution of hydraulic head (H [L]) using the values of hydraulic head in the neighboring four grid cells; and the conductivity ($K_{\rm gw}$, [L/T]) between the given cell and these four neighbors We solve this equation for interior cells:

$$\begin{split} H[x,y] = \; & ((H[x+1,y] \times K_{gw} + H[x,y+1] \times K_{gw} + H[x-1,y] \\ & \times K_{gw} + H[x,y-1] \times K_{gw}))/(K_{gw} \times 4) \end{split} \tag{2}$$

We note that this is a highly simplified expression which is only valid for isotropic, homogeneous conductivity and grid cells of equal size in *x* and *y*. The fixed head condition along the left boundary gives:

$$H_L = 0 \tag{3}$$

for cells along this boundary. The bottom and top boundaries of the model grid are set as zero flux boundaries.

$$H_{B}[x,1] = H[x,0]$$
 (4)

$$H_{\mathsf{T}}[x,ny] = H[x,ny+1] \tag{5}$$

This ensures that no flow is directed into the domain or leaves the system out of these boundaries. We impose a fixed flux of groundwater, Q_r [L³/T] into the domain along the right boundary

$$H_{R}[1,y] = (Q_{r}/(K_{gw} \times L)) + H[0,y]$$
 (6)

At the beginning of the simulation, the groundwater emerges as surface water at cells along the left side of the boundary which has an initial elevation of 0 m. In subsequent time steps we identify cells eroded to elevations of 10 m or lower. These cells are designated as seeps and the groundwater head in these cells is fixed at 0.

$$H[x_{\text{seep}}, y_{\text{seep}}] = 0 \tag{7}$$

where $[x_{seep}, y_{seep}]$ is a coordinate pair for a cell designated as a seep due to its elevation being at or below 10 m. Seeps are points of fixed head within the domain and influence the head values of the rest of the domain. Equation 2, subject to the constraints of Equations 3–7 and evolving internal locations of fixed hydraulic head, is solved iteratively until convergence is achieved for the steady-state distribution of head across the domain. Convergence is based on a tolerance criteria of < 10^{-7} [L] maximum difference in head at any cell between subsequent iterations.

Once the head field is at steady state, the volumetric flux of groundwater ($Q_{\rm gw}$, [L³/T]) to the surface in each seep cell is again calculated using Darcy's Law:

$$Q_{gw} = K_{gw} \times CA \times (|\Delta H_{left}| + |\Delta H_{right}| + |\Delta H_{up}| + |\Delta H_{down}|)$$
 (8)

where $K_{\rm gw}$ is hydraulic conductivity [L/T], CA is the cross-sectional area of the conductive layer [L²] and $\Delta H_{\rm left}$, is the dimensionless head gradient between the seep and its neighbor to the left, $\Delta H_{\rm right}$, $\Delta H_{\rm up}$, and $\Delta H_{\rm down}$ are likewise the head gradients to the other three neighbors.

The flux of groundwater to seeps is added to the accumulated precipitation and fluvial erosion is calculated according to Equation 1. The landscape is eroded for the 1000-year FastScape timescale and SeepCharge is subsequently run on the new topography to determine the new groundwater head and fluxes. We note that groundwater is routed only in four directions, unlike the D8 routing of surface water. Given that the groundwater head surface must vary smoothly in our formulation and is strongly conditioned to flow along one of the four

routing directions, we do not expect that groundwater routing would be substantially different under D8 routing.

3 | RESULTS

First, we describe the evolution of a no-routing case with 30% of water allocated to groundwater (NR-GW30) to illustrate the behavior of our coupled model for groundwater flow and landscape evolution (Figure 3). At the start of the simulation, the steady-state flow of groundwater creates a uniform seep along the left edge of the domain discharging into the boundary cells with fixed elevation. Erosion of tributaries into the valley wall initially occurs only where the random initial topography focuses the drainage from several cells together: over the majority of the domain the threshold combination of slope and discharge is not met, so no erosion occurs (Equation 1). Where erosion is supported, channels incise to 10 m elevation, at which point they become groundwater seeps and erode much more quickly as a

result of the additional discharge. After 1000 years of evolution, a set of straight and deeply eroded channels (typically eroded below 5 m elevation), spaced ~ 30 –40 m apart have formed perpendicular to the left edge of the domain (Figure 4).

At each channel head, groundwater head gradients from right to left are steeper above channel heads than above interfluves and each channel head redirects head gradients from the neighbors immediately above and below, concentrating groundwater seeps into cells along the escarpment front (Figure 5). As evolution continues, the channels capturing larger surface water drainage areas out-compete other channels and grow longer. The channels that propagate farthest to the right generate larger head gradients that extend across multiple cells and focus more groundwater. The number of significant channels decreases by about one-third so that after 100,000 years of evolution the major channels are spaced at $\sim\!50\text{--}60$ m, nearly double the initial spacing of $\sim\!30$ m.

The fraction of total water added to the system as groundwater has an impact on both the rate of landscape evolution and the

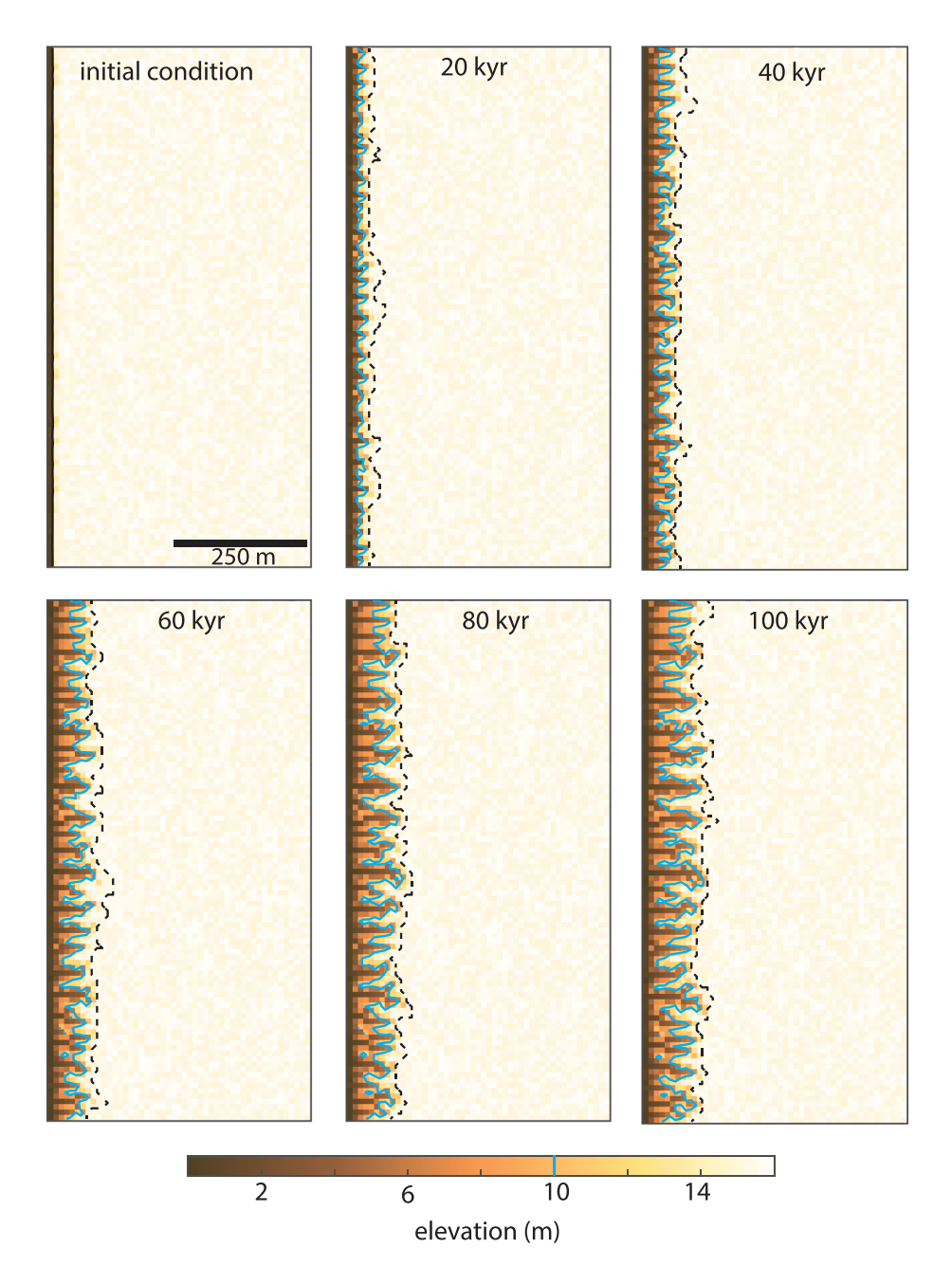


FIGURE 3 Evolution of the NR30 case for 100 kyr. Surface water falling on closed depressions and their catchments is lost to evapotranspiration and 30% of the total water is introduced as a fixed flux of groundwater in through the right edge of the model. Panels show map view images of the left half of the model domain with elevations given by the color bar below. In the initial condition an incised valley is present on the left edge of the domain. Subsequent panels show the evolution in 20 kyr increments with a dashed black line marking the evolution surface drainage divide. A blue line marks the contour of 10 m elevation where groundwater becomes surface water. After 100 kyr of evolution a series of short, straight, deeply incised channels are present

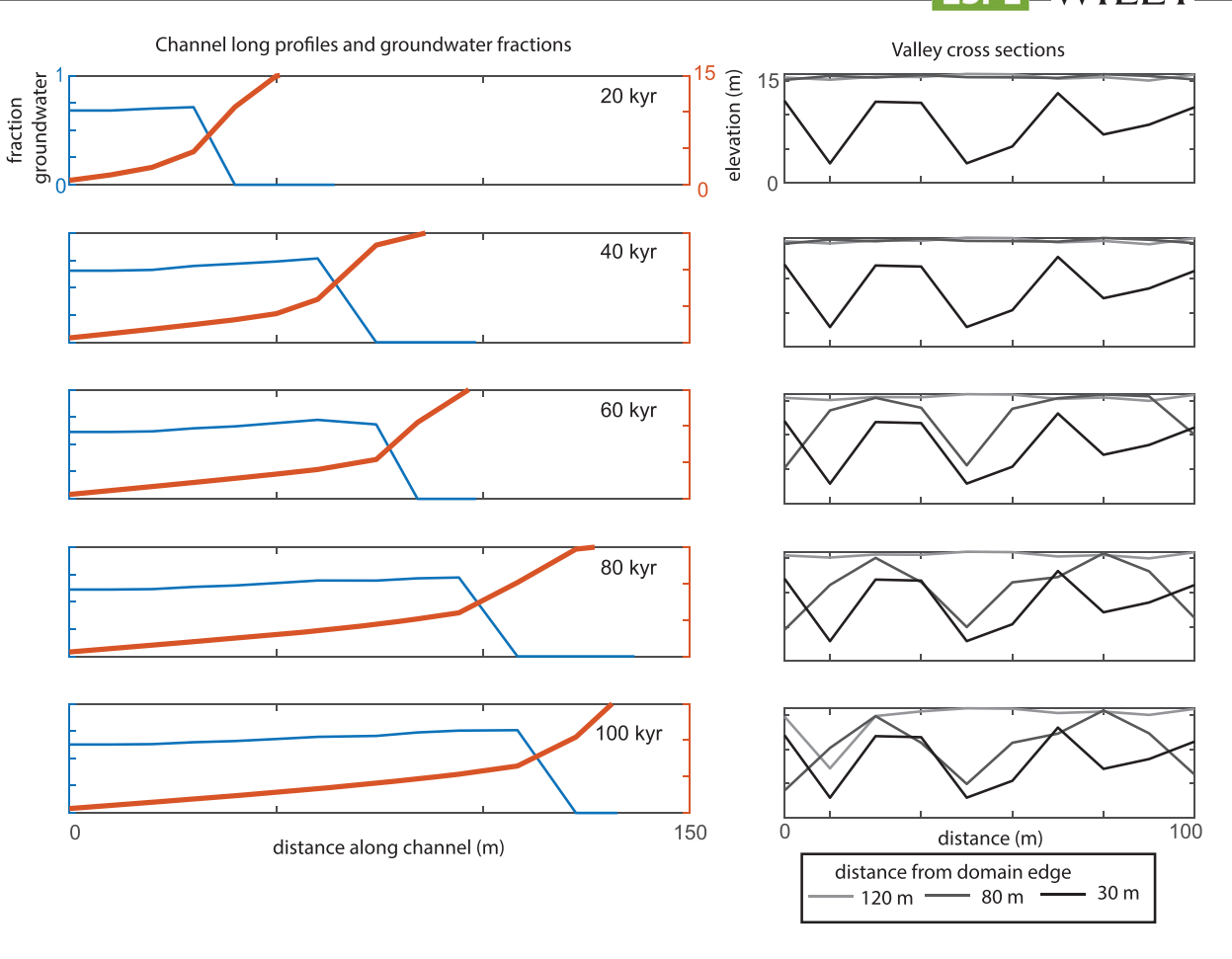


FIGURE 4 Evolving long profiles and valley cross-sections for the longest channel in case NR30. Long-profiles of the longest channel are shown in red. The fraction of the river discharge derived from groundwater is shown in blue. Where channels have eroded below 10 m elevation groundwater becomes the dominant fraction of the discharge. While groundwater is only 30% of the total water introduced to this model, it accounts for \sim 70% of the discharge in the longest channel along much of its length. Channels steepen above the point of groundwater discharge. Valley cross-sections reveal narrow, deeply-incised channels that separate high interfluves

morphology of the channel network in our model. NR-GW30 is compared to cases with fractions of groundwater ranging from 0% (NR-GW0) to 90% (NR-GW90) of the total water (Figure 6). Without groundwater, the channels grow more slowly and remain straight and closely spaced after 50 kyr. Channel long profiles have a more uniform curvature and channels are less deeply carved in the landscape in NR-GWO than in cases with groundwater contributions (Figure 7). The most rapid evolution is seen in NR-GW30. When groundwater is greater than 30% of the total water, channel long profiles show more abrupt changes in slope associated with the addition of seep water. NR-GW60, NR-GW70 and NR-GW80 have straighter channels with more uniform lengths than NR-GW10 through NR-GW50. Additionally in these high groundwater cases, the groundwater is evenly distributed to each channel head and limited surface water diminishes the impact of surface water drainage area capture. NR-GW90 has limited growth of channels due to the lack of surface water available to drive incision of a depth great enough to access groundwater. Branching of channels is generally limited in the no-routing cases but is more common with moderate groundwater contribution (10-60% of total water) than with very little or very large groundwater contributions. The combination of surface water and groundwater is important because growing channels receive a significant initial contribution from surface water that allows early development which then allows

access to groundwater. Channel-interfluve relief increases with increasing groundwater fraction, reflecting the large increases in erosional energy that result from accessing large groundwater fluxes (Figure 8).

Surface water routing speeds stream development rates relative to no-routing cases, similar to the finding of Lai and Anders (2018) for surface-water only evolution. The channel network morphology in cases with forced routing of surface water is very different than in norouting cases: routing causes the growth of a smaller number of dendritic channels with a spacing of about 200 m between channels (Figure 9). Superimposed on the dramatic difference in rates of evolution and channel morphology between routing and no-routing cases is the signature of groundwater contributions. Channel long profiles steepen and shorten with increasing fractions of groundwater (Figure 10). Deeply incised valleys propagate farther into the domain with the addition of groundwater than in its absence as can be seen by comparing the long profiles of R-GW30 and R-GW40 to R-GW0 (Figures 7 and 10). As groundwater contribution grows, the surface water routing pathways that dictate the channel pattern in R-GWO are less clearly expressed in R-GW70 through R-GW90. The position of the longest channel varies with groundwater fraction (Figure 9). This change in relative channel growth represents a softening of the extreme sensitivity to initial conditions which is a common

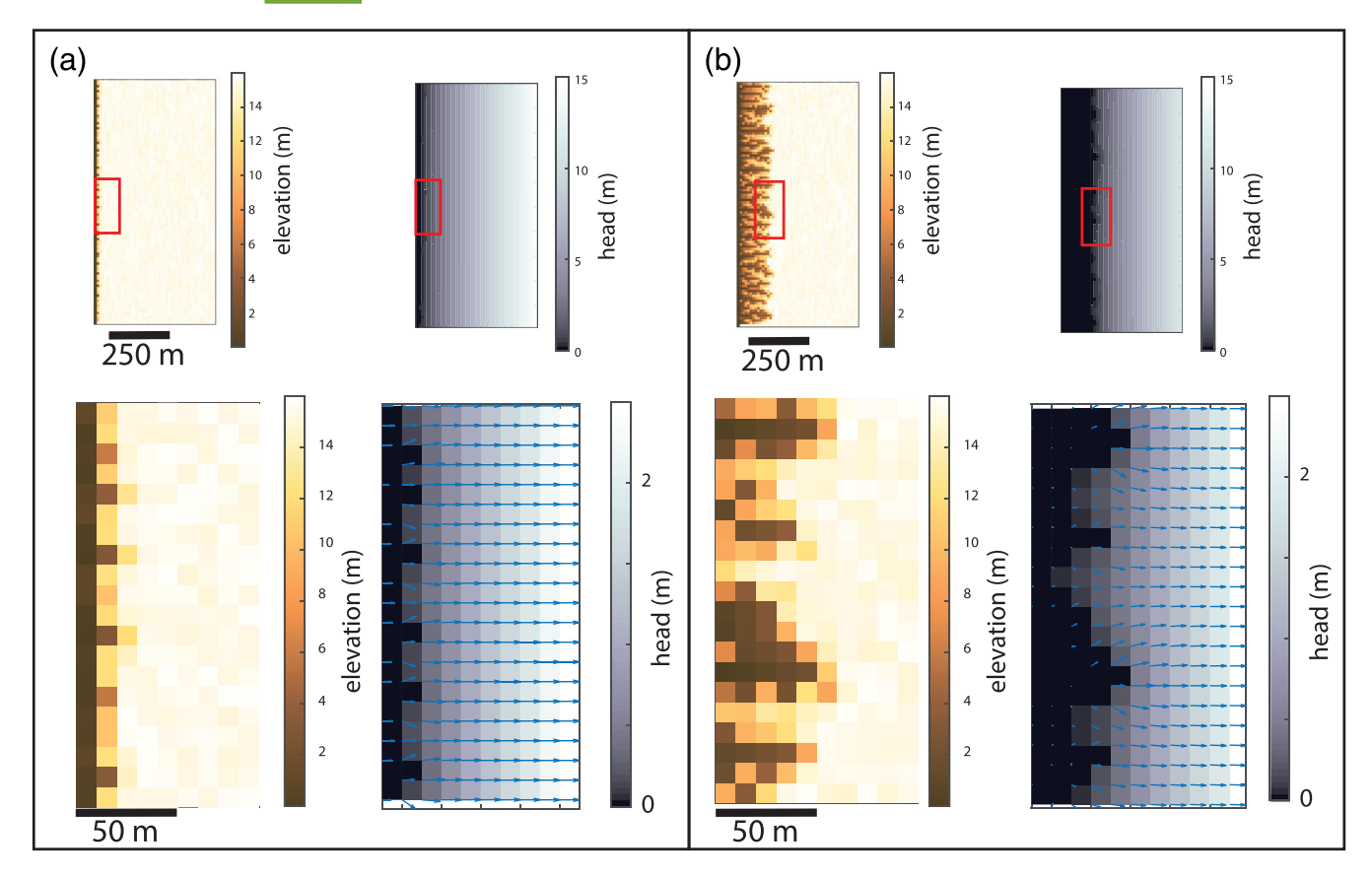


FIGURE 5 Co-evolution of the topography and the groundwater head fields. The top row shows the elevation on the left and groundwater head on the right for the entire domain after one time step (panel A) and after 100 kyr of evolution (panel B) under the NR30 scenario. The lower panels show enlarged portions of the topography on the left and head field on the right with arrows indicating the up-gradient direction. Early in the evolution (panel A) the groundwater head field indicates that flow is almost entirely flowing toward the valley wall, with water from only three pixel-widths (30 m; 3% of incoming groundwater flux) contributing to each channel head. After 100 kyr of evolution (panel B) some channel heads have out-competed others and the groundwater flow is concentrated into channel heads from across larger areas (~60 m in width, 6% of incoming groundwater flux)

(and undesirable) feature of landscape evolution models (e.g., Kwang & Parker, 2019).

4 | DISCUSSION

4.1 | Application to post-glacial landscapes

Our research was motivated by the apparent paradox of the inferred expansion of stream networks in the Central Lowlands following deglaciation despite the low relief landscape and frequent occurrence of closed depressions. Lai and Anders (2018) argue that developing stream networks in the Central Lowlands would not have had sufficient energy to grow to the observed extent without contributions of water from upland closed depressions and their catchments. They model a scenario in which upland closed depressions are connected to external drainage networks by filling lakes to their spill point and routing the overflow across the landscape. Based on our models, we propose that instead of being routed over the surface, water from upland closed depressions could have been routed to external drainage networks via the subsurface. Our numerical models suggest that drainage network growth assisted by moderate fractions of groundwater should be accelerated relative to both cases with no groundwater and cases dominated by groundwater. This maximum channel growth rate

at moderate groundwater fraction holds for both routing and norouting cases. Channel headcutting is facilitated by a step-change in discharge near the channel head that produces a steeper than expected channel gradient. This steepened reach near the channel head is a robust morphological signature of groundwater contribution in our model that could be a target for a field study of channel evolution in this region.

Our modeled landscapes can serve as a guide to field investigation of channel network histories in the region. While the groundwater flow in our model is highly idealized, we can use the morphology of channel networks in our model to identify areas in which groundwater contributions to channel development are likely. Groundwater flow in the spatially-heterogeneous glacial sediments of the Central Lowlands is influenced by strong lateral and vertical contrasts in permeability which influence flow paths for both confined and unconfined aquifers (e.g., Hinton et al., 1993; Yager et al., 2019). The geologic history and the present modeling results lead us to suspect that variability in groundwater routing related to the geometry of glacial sedimentary deposits played a role in the evolution of channel networks in the Central Lowlands. The complex history of anthropogenic alterations to the hydrology and channel networks of the Central Lowlands complicates field study of channel networks. However, our results can be used to guide selection of channels with good potential as future case study locations.

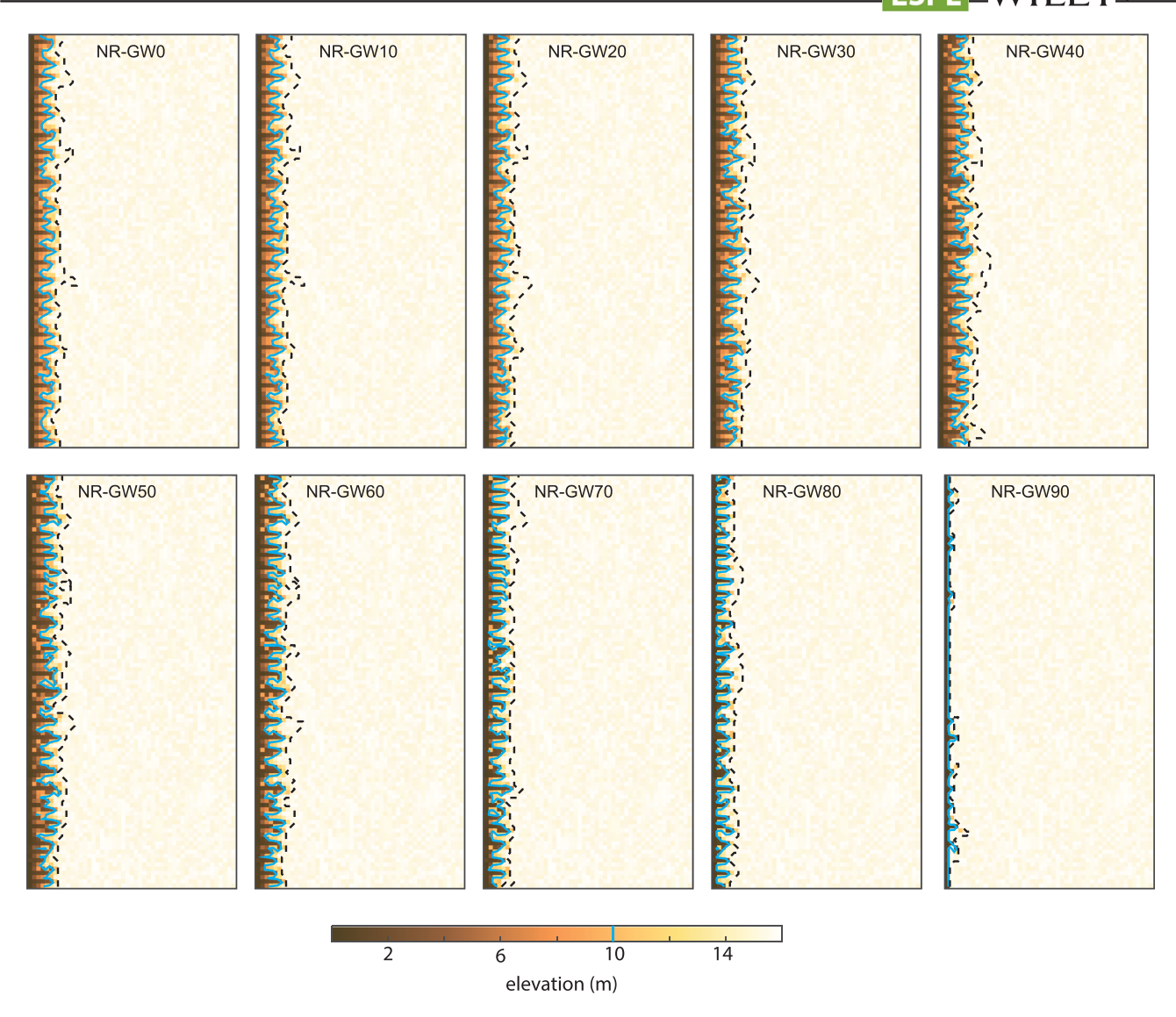


FIGURE 6 Map view of topography after 50 kyr evolution for no-routing (NR) cases with groundwater contributions of 0% to 90% of the total water with elevations indicated by the color bar. The blue contour line at 10 m elevation indicates the point at which groundwater is converted to surface water and begins to do work on the landscape. Note that the maximum migration of the 10 m elevation contour to the right is observed in moderate groundwater contribution cases (20–40%). In all cases except 90% groundwater channels remain closely spaced and uniform in length after 50 kyr evolution. A model run with 100% of water as groundwater has insufficient stream power for incision at every cell and does not evolve

4.2 | Comparison with observations and models of groundwater-dominated systems

Our models of mixed groundwater and surface water derived discharge can be compared to previous work focused on groundwater-dominated systems. In contrast to our model, groundwater is the dominant flux of water in these systems, with little to no overland flow. A groundwater-dominated hydrology is reasonable for some recently glaciated low-relief landscapes, for example, in the sandy lowlands of the Netherlands (De Vries, 1994), but where till is common at or near the surface, we expect both surficial runoff and groundwater contributions to discharge. Drainage networks formed entirely by groundwater-derived discharge in the Florida panhandle are characterized by steep-walled valleys, low-slope valley floors, long trunk streams with stubby tributaries, amphitheater-shaped valley heads (Abrams et al., 2009; Schumm et al., 1995), and a characteristic branching angle of 72° (Devauchelle et al., 2012). Amphitheater-

shaped headwalls are also characteristic of channel heads formed in weathered saprolite in the Luquillo Mountains of Puerto Rico (Harrison et al., 2020). Our models reproduce a subset of the features associated with groundwater-dominated fluvial networks (steepwalled valleys, low-slope valley floors, and long trunks with stubby tributaries) under both surface-water routing conditions (no routing of surface water out of closed depressions and complete routing of surface water out of closed depressions). As the fraction of channel water sourced from groundwater increases in our models, these characteristics become more pronounced (Figures 6 and 9). The characteristics captured by our models are replicated in physical experiments (Howard & McLane, 1988) and previous numerical models (e.g., Schumm et al., 1995). Groundwater in our model only does work on the landscape by being added to surface water in channel networks. Therefore, the characteristics we reproduce from these groundwater-dominated systems only require the spatial patterns of water accumulation present in our model and not distinct processes

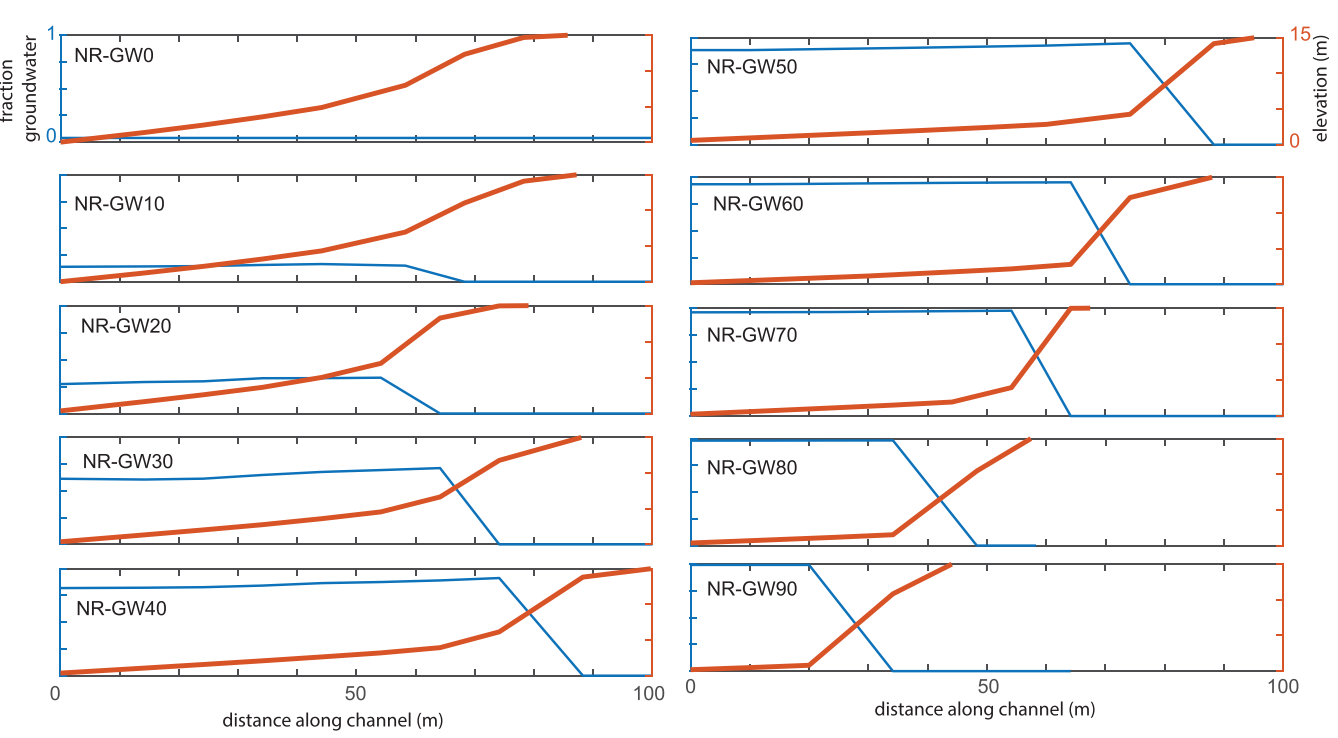


FIGURE 7 Long profile of the longest channel in each of the no-routing (NR) cases shown in thick red lines with elevation values on the right axis. Fraction of discharge in this channel from groundwater shown as thin blue line with values on the left axis. Channel length is longest for NR-GW40 and NR-GW50. In these cases the combination of groundwater and surface water is optimal to concentrate discharge. The nogroundwater case NR-GW0 has a more gently sloping channel than other cases and channels steepen significantly as groundwater is increased. For groundwater contributions greater than 50% of total water the growth of channels decreases with increasing groundwater contributions. As groundwater contribution overall increases, the fraction the discharge derived from groundwater increases. This is not proportional to the overall groundwater in the model however: for groundwater contributions of 30% and greater, the discharge in the largest channel is more than proportionally derived from groundwater (see also Figure 4)

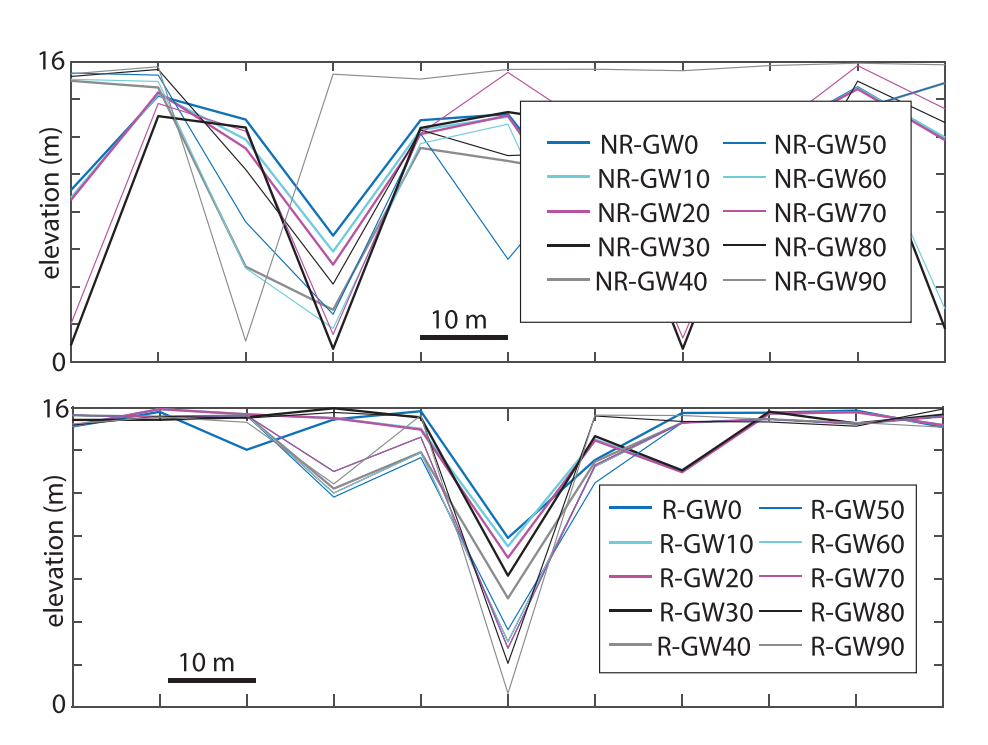


FIGURE 8 Cross-sections of topography showing ridge-valley relief for the no-routing (top panel) and routing (bottom panel) simulations after 50 kyr evolution. For each simulation a cross-section was taken for the largest channel at the point where the channel bottom elevation first dips below 10 m. Ridge-valley relief at this point increases with increasing groundwater fraction. The increased discharge in the stream from groundwater contributions causes the stream channel to incise. Compare with long profiles of the longest channels in Figures 7 and 10

of subsurface groundwater erosion. Specifically, they require large stepwise increases in discharge at the point of groundwater contribution. Emergence of groundwater at the surface drives rapid erosion in analog experiments (Howard & McLane, 1988) and channel head propagation rates are successfully modeled as a linear function of the groundwater flux (Abrams et al., 2009). Other features of

groundwater-dominated systems including the characteristic branching angle of groundwater-formed stream networks (Devauchelle et al., 2012) and the amphitheater-shaped valley heads (Abrams et al., 2009; Schumm et al., 1995) are not reproduced by our model. This suggests that more specific representation of erosion by groundwater near the channel head is needed to produce these

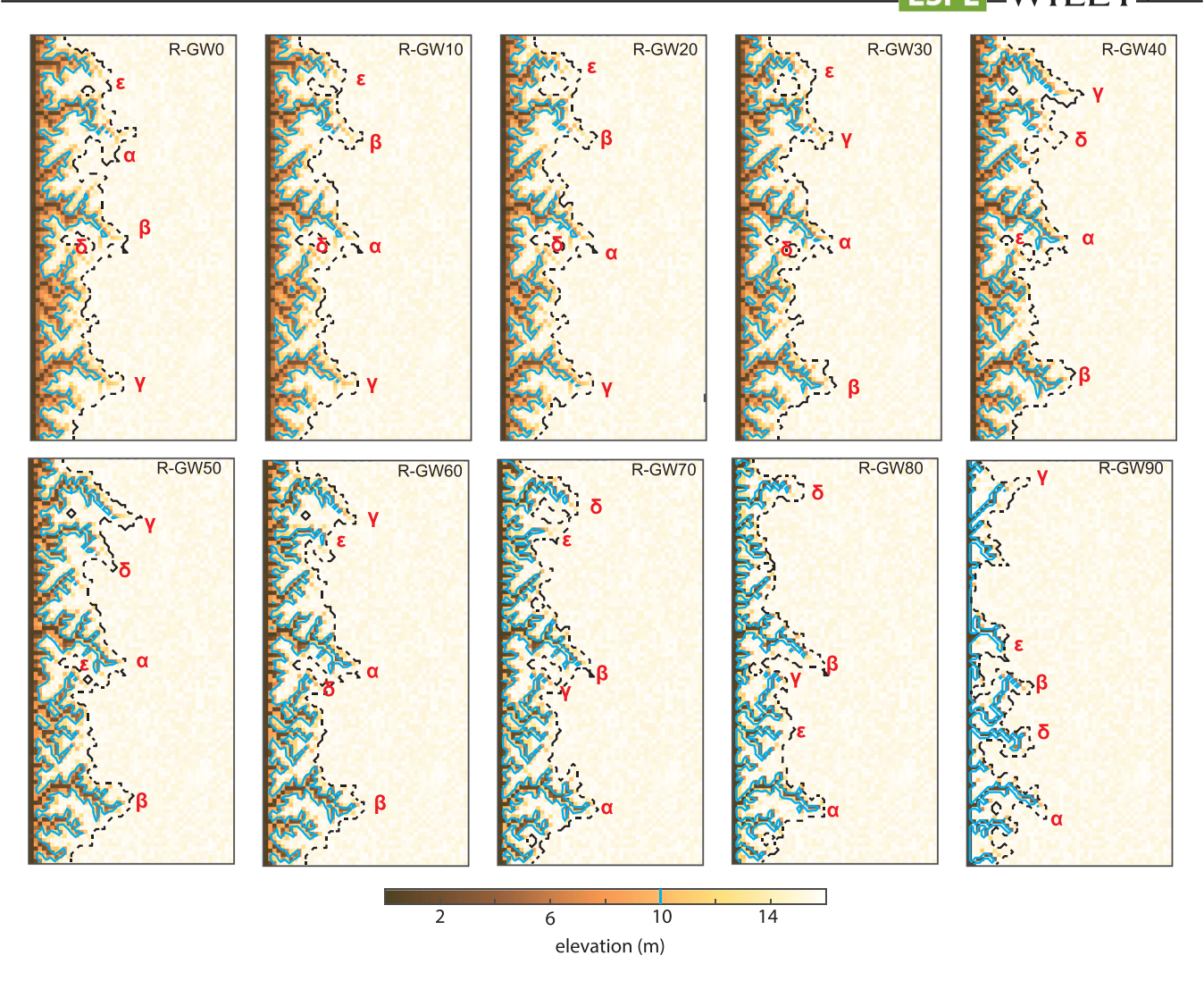


FIGURE 9 As in Figure 5 but for routing (R) cases. Overall growth of the channel network after 50 kyr is much greater than in no-routing (NR) cases (Figure 6). Under routing conditions a smaller number of channels grow long. The longest five channels in each simulation are marked with α , β , γ , δ , and ϵ in order. The initial random seed of the topography is held constant in all simulations. However, increasing groundwater contributions are able to change the competition between different channels, overcoming the sensitive dependence on initial conditions. As in NR cases, the greatest propagation of the channel head is observed in cases with moderate groundwater contributions (20–50% of the total water as groundwater). Branching generally diminishes with groundwater contributions greater than \sim 60%

features and/or the spatial resolution of our model (10 m) is insufficient to resolve these structures.

Our model features competition between channels to capture groundwater which drives incision and subsequent capture of surface area, as can be seen in the differential extension of channels modeled with different groundwater fractions but the same initial random topography (Figures 6 and 9). Channel extension occurs through the capture of internally-drained closed depressions in our model. Field observations in Puerto Rico suggest that groundwaterdriven channel network extension is a significant driver of capture events that reorganize an upland stream network (Harrison et al., 2020). In Puerto Rico the progressive weathering of bedrock to produce a permeable layer of saprolite was required for groundwater to become a significant driver of stream hydrology and erosion (Harrison et al., 2020). The layering of different materials in the postglacial Central Lowlands similarly produces horizontal contrasts in permeability (Anders et al., 2018), favoring horizontal groundwater flow paths and allowing for groundwater emergence at relatively shallow depths of incision.

4.3 | Broader relevance to landscape evolution and hydrologic modeling

Our interest in developing different representations of hydrology for use in landscape evolution modeling is shared by a larger community and more sophisticated representations of hydrology are actively being developed for landscape evolution models. For example, the module GroundwaterDupuitPercolator was developed for Landlab to simulate flow in an unconfined aquifer (Litwin et al., 2020). Future work on the hydrology of the Central Lowlands could incorporate this component to simulate two-way transfer of water between the surface and subsurface in areas of low relief. Motivated in part by the landscapes of the Central Lowlands, FlowFill (Callaghan & Wickert, 2019) and Fill-Spill-Merge (Barnes et al., 2020) are two new algorithms for handling flow routing in areas with surface depressions. Instead of routing water out of all closed depressions through the lowest point along the basin boundary as in Tucker et al. (2001), these algorithms specify a surface runoff depth and fill only those depressions which would be flooded by this amount of runoff. This has the

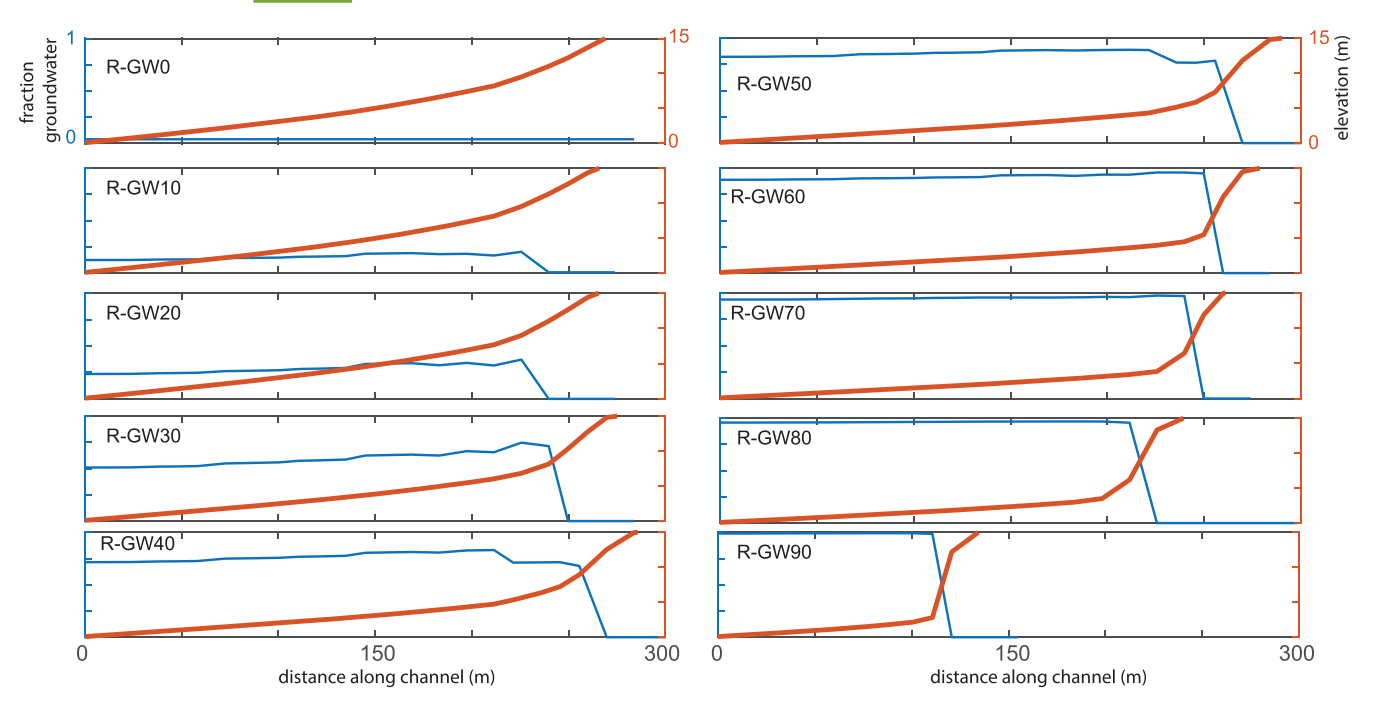


FIGURE 10 Long profiles of the long channel in the middle of the domain in bold red and elevation values on the right axis. Fraction of the discharge derived from groundwater in the thin blue line with values on the left axis. Note that channels are much longer than in no-routing (NR) cases (compare Figure 7). Groundwater contribution to this large channel is greater than the overall fraction of groundwater in the domain for R-GW30 through R-GW90. Channel steepen below the point of groundwater discharge (10 m). As in no-routing cases, the greatest channel lengths are associated with moderate values of groundwater

advantage of mass conservation for water and differential connectivity of depressions as a function of their size, depth and position which is more physically reasonable than the end-member scenarios we consider. We hypothesize that the long-term evolution of a low-relief landscape with flow routing dictated by FlowFill or Fill-Spill-Merge would be intermediate between the routing and no-routing scenarios presented here and in Lai and Anders (2018). Testing of this hypothesis is a target for future work.

Landscape evolution models commonly show extreme dependence on initial conditions (e.g., Hancock, 2006; Ijjász-Vásquez et al., 1992). For example, small differences in the topographic initial condition result in different planform geometry of river networks forming on an unchannelized area (Ijjász-Vásquez et al., 1992: Kwang & Parker, 2019; Perron & Fagherazzi, 2012). The difference in topography over time between two simulations with slightly different initial conditions was found to grow as a power-law function of time during early evolution by Ijjász-Vásquez et al. (1992). Statistical properties of landscapes, for example, the mean and variability of channel spacing (Perron & Fagherazzi, 2012), are not sensitive to small perturbations in the initial condition. In addition to this sensitivity to the initial condition, many numerical simulations of channel network evolution tend toward a time-invariant steady-state (e.g., Tucker & Slingerland, 1994; Willgoose et al., 1991), which contrasts with observations suggesting ongoing evolution of drainage divides in natural systems even in the absence of tectonic forcing (e.g., Beeson et al., 2017). Kwang and Parker (2019) demonstrate that numerical landscapes eroded by the stream-power based fluvial erosion law with steepest descent flow routing retain a memory of the noise of the initial condition in the planform of the channel network throughout their evolution (Kwang & Parker, 2019). They note that channel network planform geometry is set by the initial routing of water across a noisy surface and is very difficult to overcome (Kwang & Parker, 2019). Pelletier (2004) showed that models using bifurcation routing, in which flow is distributed to all downslope neighboring grid points, retained persistent divide migration over timescales an order of magnitude longer than those required to reach steady-state in steepest-descent routing cases. By introducing a dependence on the detailed shape of topography, rather than just the topological ordering of grid points, bifurcation routing induces autogenic variability into the topographic evolution (Pelletier, 2004). Our introduction of groundwater similarly introduces an additional degree of freedom for evolution of the landscape, reducing the dependence on surface drainage area and the associated algorithm for routing water out of closed depressions and allowing the details of the initial condition to be erased from the drainage network.

We emphasize that there has been a substantial body of work exploring how relaxation of a rigid coupling of drainage area (as calculated from a topographic surface using simple flow-routing algorithms) and river discharge influences numerical landscape evolution models. For example, previous work exploring the impact of spatial variability in precipitation due to interactions with topography (e.g., Anders et al., 2008; Colberg & Anders, 2014; Han et al., 2015; Huang & Niemann, 2014) and temporal variability in precipitation driven by weather events (e.g., DiBiase & Whipple, 2011; Lague et al., 2005; Molnar et al., 2006; Tucker & Bras, 1998), introduce factors other than surface drainage area as important drivers of variability in discharge, and, therefore, fluvial erosion rates. Landscape evolution modeling requires simplification and idealization. We suggest that, for consideration of some settings including low-relief un-channelized areas, the idealization of discharge as a direct scaling of surface drainage area can and should be replaced with other appropriate representations of hydrology.

5 | CONCLUSION

Fluvial channels form and propagate in unchannelized low relief areas. Where slopes are low, the energy required for channel incision must be generated by spatially-concentrated discharge. Previous work has recognized that water can be concentrated in low-relief landscapes by filling, and then spilling out of, closed depressions. We propose another potential mechanism for spatially concentrating water in low relief settings: the convergence and emergence of shallow groundwater at channel heads. Groundwater flow paths may cross subtle surface water divides and thus supply water beyond what is directly precipitated onto the local land surface.

Incising channels alter groundwater head gradients, potentially routing groundwater to channel heads from beyond their surface water catchment boundaries. Groundwater contributions also produce distinctive morphology including steepened channel profiles below groundwater seeps and diminished branching with large groundwater contributions. Groundwater head gradients evolve with topography and groundwater-fed channels can grow more quickly than channels with larger surface water catchments. We conclude that groundwater may have a significant and recognizable impact on channel network evolution in low-relief areas. Additionally, our work prompts examination of conceptual models of flow routing and accumulation used in fluvial landscape evolution modeling. In particular, we note that a representation of groundwater derived from beyond surface basin boundaries reduces the dependence of modeled fluvial networks on the details of the initial topography. In comparing our models to groundwater dominated landscapes, we find that the large discrete increases in discharge due to groundwater emergence reproduce some of the morphological features of these landscapes without the inclusion of groundwaterspecific erosion mechanisms. Most importantly, our model suggests key morphologic features created by groundwater contributions to stream networks that can serve as targets for future field investigation.

DATA AVAILABILITY STATEMENT

Scripts and notebooks used in this study can be found and cited at 10. 5281/zenodo.5567312

ORCID

Cecilia Cullen https://orcid.org/0000-0003-4969-7112

Alison M. Anders https://orcid.org/0000-0002-7597-5465

Jingtao Lai https://orcid.org/0000-0001-9745-150X

Jennifer L. Druhan https://orcid.org/0000-0003-0200-3988

REFERENCES

- Abrams, D.M., Lobkovsky, A.E., Petroff, A.P., Straub, K.M., McElroy, B., Mohrig, D.C. et al. (2009) Growth laws for channel networks incised by groundwater flow. *Nature Geoscience*, 2, 193–196. https://doi. org/10.1038/ngeo432
- Anders, A.M., Bettis, E.A., III, Grimley, D.A., Stumpf, A.J. & Kumar, P. (2018) Impacts of Quaternary history on critical zone structure and processes: Examples and a conceptual model from the intensively managed landscapes critical zone observatory. Frontiers in Earth Science, 6, 24. 10.3389/feart.2018.00024.
- Anders, A.M., Roe, G.H., Montgomery, D.R. & Hallet, B. (2008) Influence of precipitation phase on the form of mountain ranges. *Geology*, 36(6), 479–482.
- Anderson, R.S. (1994) Evolution of the Santa Cruz Mountains, California, through tectonic growth and geomorphic decay. *Journal of*

- Geophysical Research Solid Earth, 99(20), 161-179. https://doi.org/10.1029/94JB00713
- Anderson, R.S., Densmore, A.L. & Ellis, M.A. (1999) The generation and degradation of marine terraces. *Basin Research*, 11(1), 7–19. https://doi.org/10.1046/j.1365-2117.1999.00085.x
- Barnes, R., Callaghan, K.L. & Wickert, A.D. (2020) Computing water flow through complex landscapes – Part 2: Finding hierarchies in depressions and morphological segmentations. *Earth Surface Dynamics*, 8, 431–445. https://doi.org/10.5194/esurf-8-431-2020
- Barnhart, K.R., Hutton, E.W.H., Tucker, G.E., Gasparini, N.M., Istanbulluoglu, E., Hobbley, D.E.J. et al. (2020) Short communication: Landlab v2.0: A software package for Earth surface dynamics. *Earth Surface Dynamics*, 8(2), 379–397. https://doi.org/10.5194/esurf-8-379-2020
- Beaumont, C., Fullsack, P. & Hamilton, J. (1992) Erosional control of active compressional orogens. In: McClay, K.R. (Ed.) *Thrust Tectonics*. New York: Chapman and Hall, pp. 1–18.
- Beeson, H.W., McCoy, S. & Keen-Zebert, A. (2017) Geometric disequilibrium of river basins produces long-lived transient landscapes. *Earth and Planetary Science Letters*, 475, 34–43. https://doi.org/10.1016/j.epsl.2017.07.010
- Blair, N., Hayes, J.M., Grimley, D. & Anders, A.M. (2021) Eroded Critical Zone Carbon and where to find it: Examples from the IML-CZO. In: Wymore, A.S., Yang, W.H., Silver, W., McDowell, W.H. & Chorover, J. (Eds.), Biogeochemistry of the Critical Zone. Advances in Critical Zone Science. Cham, Switzerland: Springer Nature Switzerland AG. In press.
- Braun, J. & Willett, S. (2013) A very efficient O(n), implicit and parallel method to solve the stream power equation governing fluvial incision and landscape evolution. *Geomorphology*, 180–181, 170–179. https://doi.org/10.1016/j.geomorph.2012.10.008
- Callaghan, K.L. & Wickert, A.D. (2019) Computing water flow through complex landscapes – Part 1: Incorporating depressions in flow routing using FlowFill. Earth Surface Dynamics, 7(3), 737–753. https:// doi.org/10.5194/esurf-7-737-2019
- Colberg, J.S. & Anders, A.M. (2014) Numerical modeling of spatially-variable precipitation and passive margin escarpment evolution. *Geomorphology*, 207, 203–212. https://doi.org/10.1016/j.geomorph. 2013.11.006
- Cuthbert, M. Ph.D. dissertation, University of Birmingham, United Kingdom
- De Vries, J.J. (1976) The groundwater outcrop-erosion model; evolution of the stream network in the Netherlands. *Journal of Hydrology*, 29(1–2), 43–50. https://doi.org/10.1016/0022-1694(76)90004-4
- De Vries, J.J. (1994) Dynamics of the interface between streams and groundwater systems in lowland areas, with reference to stream net evolution. *Journal of Hydrology*, 155(1–2), 39–56. https://doi.org/10. 1016/0022-1694(94)90157-0
- Devauchelle, O., Petroff, A.P., Seybold, H.F. & Rothman, D.H. (2012) Ramification of stream networks. *Proceedings of the National Academy of Sciences of the United States of America*, 109(51), 20832–20836. https://doi.org/10.1073/pnas.1215218109
- DiBiase, R.A. & Whipple, K.X. (2011) The influence of erosion thresholds and runoff variability on the relationships among topography, climate, and erosion rate. *Journal of Geophysical Research Earth Surface*, 116, F04036. https://doi.org/10.1029/2011JF002095
- Dunne, T. (1980) Formation and controls of channel networks. *Progress in Physical Geography*, 4(2), 211–239. https://doi.org/10.1177/030913338000400204
- Fenneman, N.M. & Johnson, D.W. (1946) Physiographic divisions of the conterminous US. Reston, VA: United States Geological Survey.
- Hancock, G.R. (2006) The impact of different gridding methods on catchment geomorphology and soil erosion over long timescales using a landscape evolution model. *Earth Surface Processes and Landforms*, 31(8), 1035–1050. https://doi.org/10.1002/esp.1306
- Han, J., Gasparini, N.M. & Johnson, J.P.L. (2015) Measuring the imprint of orographic rainfall gradients on the morphology of steady-state numerical fluvial landscapes. *Earth Surface Processes and Landforms*, 40(10), 1334–1350.
- Harrison, E.J., Brocard, G.Y., Gasparini, N.M., Lyons, N.J. & Willenbring, J. K. (2020) Seepage erosion in the Luquillo Mountains, Puerto Rico,

- Relict Landscapes. Journal of Geophysical Research Earth Surface, 125(6), e2019JF005341. https://doi.org/10.1029/2019JF005341
- Higgins, C.G. (1984) Piping and sapping: Development of landforms by groundwater outflow. Groundwater as a geomorphic agent. London: Routledge.
- Hinton, M.J., Schiff, S.L. & English, M.C. (1993) Physical properties governing groundwater flow in a glacial till catchment. *Journal of Hydrology*, 142(1–4), 229–249. https://doi.org/10.1016/0022-1694 (93)90012-X
- Hobley, D.E.J., Adams, J.M., Nudurupati, S.S., Hutton, E.W.H., Gasparini, N.M., Istanbulluoglu, E. & Tucker, G.E. (2017) Creative computing with Landlab: An open-source toolkit for building, coupling, and exploring two-dimensional numerical models of Earth-surface dynamics. *Earth Surface Dynamics*, 5(1), 21–46. https:// doi.org/10.5194/esurf-5-21-2017
- Howard, A.D. & McLane, C.F. (1988) Erosion of cohesionless sediment by groundwater seepage. Water Resources Research, 24(10), 1659–1674. https://doi.org/10.1029/WR024i010p01659
- Huang, X. & Niemann, J.D. (2014) Simulating the impact of small convective storms and channel transmission losses on gully evolution. Reviews in Engineering Geology, 22, 131–145.
- Ijjász-Vásquez, E.J., Bras, R.L. & Moglen, G.E. (1992) Sensitivity of a basin evolution model to the nature of runoff production and to initial conditions. Water Resources Research, 28(10), 2733–2741. https://doi. org/10.1029/92WR01561
- Kwang, J.S. & Parker, G. (2019) Extreme memory of initial conditions in numerical landscape evolution models. Geophysical Research Letters, 46(12), 6563–6573. https://doi.org/10.1029/2019GL083305
- Lague, D. (2013) The stream power river incision model: Evidence, theory and beyond. Earth Surface Processes and Landforms, 39, 38-61. https://doi.org/10.1002/esp.3462
- Lague, D., Hovius, N. & Davy, P. (2005) Discharge, discharge variability, and the bedrock channel profile. *Journal of Geophysical Research: Earth Surface*, 111, F4. https://doi.org/10.1029/2004JF000259
- Lai, J. & Anders, A.M. (2018) Modeled Postglacial landscape evolution at the southern margin of the Laurentide Ice Sheet: Hydrological connection of uplands controls the pace and style of fluvial network expansion. *Journal of Geophysical Research - Earth Surface*, 123(5), 967–984. https://doi.org/10.1029/2017JF004509
- Le, P.V., Kumar, P., Valocchi, A.J. & Dang, H.V. (2015) GPU-based high-performance computing for integrated surface-sub-surface flow modeling. *Environmental Modelling and Software*, 73, 1–13. https://doi.org/10.1016/j.envsoft.2015.07.015
- Litwin, D.G., Tucker, G.E., Barnhart, K.R. & Harman, C.J. (2020) Groundwater Dupuit Percolator: A Landlab component for groundwater flow. *Journal of Open Source Software*, 5(46), 1935. https://doi.org/10. 21105/joss.01935
- Miller, B.A., Crumpton, W.G. & van der Valk, A.G. (2009) Spatial distribution of historical wetland classes on the Des Moines Lobe, Iowa. *Wetlands*, 29(4), 1146–1152. https://doi.org/10.1672/08-158.1
- Molnar, P., Burlando, P., Kirsch, J. & Hinz, E. (2006) Model investigations of the effects of land-use changes and forest damage on erosion in mountainous environments. In: Sediment Dynamics and the Hydromorphology of Fluvial Systems. Wallingford: IAHS Press, pp. 589-600.
- Montgomery, D.R. & Dietrich, W.E. (1995) Hydrologic processes in a lowgradient source area. Water Resources Research, 31(1), 1–10. https://doi.org/10.1029/94WR02270
- OCallaghan, J.F. & Mark, D.M. (1984) The extraction of drainage networks from digital elevation data. *Computer Vision, Graphics and Image Processing*, 28(3), 323–322. https://doi.org/10.1016/S0734-189X (84)80011-0
- Pelletier, J.D. (2004) Persistent drainage migration in a numerical landscape evolution model. *Geophysical Research Letters*, 31(20), L20501. https://doi.org/10.1029/2004GL020802
- Perron, J.T. & Fagherazzi, S. (2012) The legacy of initial conditions in landscape evolution. Earth Surface Processes and Landforms, 37(1), 52–63. https://doi.org/10.1002/esp.2205
- Pillans, B. (1985) Southwest North Island paleoenvironments 150,000 years B.P. to present, Vol. 31. Wellington: Victoria University of Wellington Geology Department Publication, pp. 38–44.

- Ruhe, R.V. (1952) Topographic discontinuities of the Des Moines lobe. American Journal of Science, 250(1), 46–56. https://doi.org/10.2475/ajs.250.1.46
- Schumm, S.A., Boyd, K.F., Wolff, C.G. & Spitz, W.J. (1995) A ground-water sapping landscape in the Florida panhandle. *Geomorphology*, 12(4), 281–297. https://doi.org/10.1016/0169-555X(95)00011-S
- Shaller, M.F. & Fan, Y. (2009) River basins are groundwater exporters and importers: Implications for water cycle and climate modeling. *Journal of Geophysical Research-Atmospheres*, 114(D4), D4. https://doi.org/10.1029/2008JD010636
- Simon, A. (1999) Channel and drainage-basin response of the Toutle River system in the aftermath of the 1980 eruption of Mount St. Helens, Washington. Washington, DC: US Department of the Interior, US Geological Survey; Branch of Distribution.
- Smith, A.P. (2007) PhD Dissertation, Indiana University. *Riparian zone hydrology and hydrogeomorphric setting of a glaciated valley in central Indiana*. http://hdl.handle.net/1805/788
- Swanson, S.K., Bradbury, K.R. & Hart, D.J. (2009) Assessing the vulnerability of spring systems to groundwater withdrawals in southern Wisconsin. *Geoscience Wisconsin*, 20, 1–13.
- Tucker, G. & Bras, R.L. (1998) Hillslope processes, drainage density, and landscape morphology. Water Resources Research, 34(10), 2751–2764. https://doi.org/10.1029/98WR01474
- Tucker, G.E., Lancaster, S.T., Gasparini, N.M. & Bras, R.L. (2001) The channel-hillslope integraded landscape development model (CHILD). In: Landscape Erosion and Evolution Modeling. Boston, MA: Springer US, pp. 349–388.
- Tucker, G.E. & Slingerland, R.L. (1994) Erosional dynamics, flexural isostasy, and long-lived escarpments: A numerical modeling study. *Journal of Geophysical Research*, 99(B6), 12,229–12,243. https://doi.org/10.1029/94JB00320
- Urban, M.A. (2005) An uninhabited waste: transforming the Grand Prairie in nineteenth century Illinois, USA. *Journal of Historical Geography*, 31(4), 647–665.
- Whipple, K.X. & Tucker, G.E. (1999) Dynamics of the stream-power river incision model: Implications for height limits of mountain ranges, landscape response timescales, and research needs. *Journal of Geophysical Research*, 104(B8), 17,661–17,674. https://doi.org/10.1029/ 1999JB900120
- Willgoose, G., Bras, R. & Rodriguez-Iturbe, I. (1991) A coupled channel network growth and hillslope evolution model: 1. Theory. Water Resources Research, 27(7), 1671–1684. https://doi.org/10.1029/91WR00935
- Winter, T.C. & Rosenberry, D.O. (1998) Hydrology of prairie pothole wetlands during drought and deluge: a 17-year study of the Cottonwood Lake wetland complex in North Dakota in the perspective of longer term measured and proxy hydrological records. *Climatic Change*, 40(2), 189–209. https://doi.org/10.1023/A:1005448416571
- Winter, T.C., Rosenberry, D.O. & La Baugh, J.W. (2003) Where does the groundwater in small watersheds come from? *Groundwater*, 41(7), 989–1000. https://doi.org/10.1111/j.1745-6584.2003.tb02440.x
- Yager, R.M., Kauffman, L.J., Soller, D.R., Haj, A.E., Heisig, P.M., Buchwald, C.A. et al. (2019) Characterization and occurrence of confined and unconfined aquifers in Quaternary sediments in the glaciated conterminous United States (ver. 1.1, February 2019): United States Geological Survey Scientific Investigations Report 2018–5091. Reston, VA: United States Geological Survey, p. 90 10.3133/sir20185091.
- Yan, Q., Le, P.V., Woo, D.C., Hou, T., Filley, T. & Kumar, P. (2019) Three-dimensional modeling of the coevolution of landscape and soil organic carbon. Water Resources Research, 55(2), 1218–1241. https://doi.org/10.1029/2018WR023634

How to cite this article: Cullen, C., Anders, A.M., Lai, J. & Druhan, J.L. (2021) Numerical modeling of groundwater-driven stream network evolution in low-relief post-glacial landscapes. *Earth Surface Processes and Landforms*, 1–14. Available from: https://doi.org/10.1002/esp.5278